

Satish G. Kandlikar<sup>1</sup>

e-mail: sgkeme@rit.edu

Wai Keat Kuan

Abhijit Mukherjee

Thermal Analysis and Microfluidics Laboratory,  
Department of Mechanical Engineering,  
Rochester Institute of Technology,  
76 Lomb Memorial Dr.,  
Rochester, NY 14623

# Experimental Study of Heat Transfer in an Evaporating Meniscus on a Moving Heated Surface

*A stable meniscus is formed by a circular nozzle dispensing water over a heated circular face of a rotating cylindrical copper block. The nozzle is offset from the axis of rotation of the copper block and thus a moving meniscus is formed on the surface. The water flow rate, heater surface temperature, and the speed of rotation are controlled to provide a stable meniscus with continuous evaporation of water without any meniscus breakup. The study provides an important insight into the role of the evaporating liquid-vapor interface and transient heat conduction around a nucleating bubble in pool boiling.*

[DOI: 10.1115/1.1857948]

## Introduction

Heat transfer at the liquid-vapor interface with a moving contact line on a heated surface is of great interest in boiling studies. The meniscus region heat transfer is not well understood, and a direct measurement of heat flux under an evaporating meniscus is useful in providing insight into the associated heat transfer phenomena. The heat transfer around a nucleating bubble is in many respects similar to the advancing and receding motion of the meniscus on a heated surface.

A novel technique is presented in this paper by which we can access the liquid-vapor interface and the contact line region (defined as the region where the liquid-vapor interface meets the heater surface). Figure 1 presents a comparison between a moving meniscus and a nucleating bubble. As the bubble grows, the liquid-vapor interface advances into the liquid; the receding liquid front of a moving meniscus represents this region of the bubble ebullition cycle. As the bubble grows to its departure size, its footprint on the heater surface rapidly shrinks as the liquid front advances over the region that formed the bubble base during the bubble growth period. This region of rewetting is represented by the advancing liquid front of a moving meniscus.

Figure 2 shows the details of a wedge of thin liquid film on a heated surface. Three regions are identified here: (i) *Nonevaporating Adsorbed Thin-Film Region*. In this region, liquid is adsorbed on the heater surface and forms a nonevaporating layer. The molecular forces have controlling influence, and the disjoining pressure reduces the pressure in the liquid and enables it to reside in a supersaturated liquid state. (ii) *Evaporating Thin-Film Region*. Evaporation occurs at the liquid-vapor interface, and liquid is fed from the bulk liquid through the intrinsic meniscus region. Here both the disjoining pressure and the capillary forces play a role. (iii) *Intrinsic Meniscus Region*. The fluid mechanics in this region is governed by the conventional equation of capillarity.

Previous studies on meniscus mainly focused on stationary menisci, which were formed inside or at the outlet end of a capillary or a small diameter tube, or at a straight edge between two intersecting surfaces. The focus of most of these studies [1–23] was the microscale and macroscale heat transfer and fluid mechanics in the vicinity of the stationary contact line region.

A clear influence of the meniscus velocity on heat flux was demonstrated in their early experiments by Kandlikar and Kuan

[24,25]. In their experiments, heat flux was found to increase linearly with the meniscus velocity from 0 to 0.38 m/s. Further increase in velocity caused a meniscus breakdown. The variation of advancing and receding contact angles with meniscus velocity was also studied over the range of parameters investigated.

The advantages of studying the meniscus geometry are fairly obvious: (i) the liquid-vapor interface and the contact line region can be viewed clearly without any obstruction from the highly active boiling phenomena occurring around a bubble in pool boiling, and (ii) under stable operating conditions, the liquid flow rate provides a direct measurement of the heat transfer rate over the wetted region bounded by the advancing and receding interfaces.

## Literature Review

As mentioned earlier, previous studies on meniscus mainly focused on stationary menisci, which were formed inside or at the outlet end of a capillary or a small diameter tube, or at a straight edge formed between two intersecting surfaces.

In 1978, Wayner [1] stated that viscous flow in a thin film in the immediate vicinity of the interline (junction of solid-liquid-vapor) significantly affects the complete profile of an evaporating meniscus. This change as a function of heat flux was theoretically analyzed based on the premise that fluid flow was caused by the London–van der Waals dispersion force. In their analysis, the change in the apparent contact angle from its intrinsic value was attributed to viscous effects only and did not include a surface roughness effect. The extended meniscus was divided into three zones: (i) the immediate vicinity of the interline (the thin film region), where the thickness of the liquid can vary from a monolayer to approximately 500 Å; (ii) the inner intrinsic meniscus region, where the thickness range is approximately  $0.05\text{--}10 \times 10^{-6}$  m; and (iii) the outer intrinsic meniscus region, where the thickness is greater than  $10^{-5}$  m.

Holm and Goplen [2] stated in 1979 that very high heat transfer rates have been observed near the triple interline, the junction of the vapor, the evaporating thin film, and the nonevaporating adsorbed thin film. Dropwise condensation was used as an example that exhibits surface heat transfer coefficients that are approximately one order-of-magnitude greater than the coefficients resulting from film condensation. At the same time, Holm and Goplen demonstrated that the extent of interline dispersion at any time can be controlled by using capillary grooves partially filled with a liquid as a means of forming the triple interline region. The heat transfer is augmented by the flow of the liquid into the groove under the action of capillary forces—a passive process. Because

<sup>1</sup>Corresponding author.

Manuscript received August 20, 2003; revision received December 15, 2004. Review conducted by: J. N. Chung.

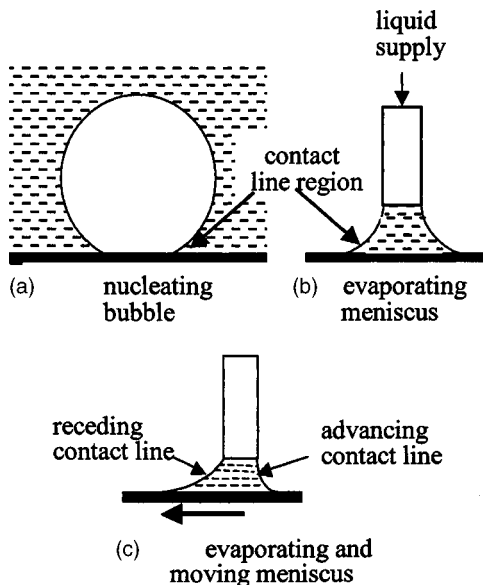


**Fig. 1 Similarity between a nucleating bubble and an evaporating meniscus in the contact line region**

of the small physical dimensions associated with a meniscus, the local characteristics of the combined heat and mass transfer processes were deduced from overall characteristics, such as (i) total heat transfer from a grooved plate, (ii) overall temperature drops in the walls separating the grooves, and (iii) the temperature difference between the top of the wall and the surrounding vapor.

In 1992, Swanson and Herdt [3] formulated a mathematical model describing the evaporating meniscus in a capillary tube incorporating the full three-dimensional Young-Laplace equation, Marangoni convection, London-van der Waals dispersion forces, and nonequilibrium interface conditions. The governing equations and boundary conditions were cast in terms of five coupled nonlinear ordinary differential equations and solved numerically. The model was tested using various values of the dimensionless superheat and dispersion number.

In 1994, Hallinan et al. [4] determined the effects of evaporation from the thin film region of a liquid-vapor meniscus within the micropores of a heat pipe wick on the interfacial shape, temperature distribution, and pressure distribution.

Khrustalev and Faghri [5] developed a mathematical model of the evaporating liquid-vapor meniscus in a capillary slot in 1996. The model consists of two-dimensional steady-state momentum conservation and energy equations for both the vapor and liquid phases and incorporates the existing simplified one-dimensional model of the evaporating microfilm. A constant wall temperature is assumed in the analysis because the solid wall thermal conductivity is significantly higher than that of liquid.

Kim and Wayner [6] experimentally and theoretically evaluated the microscopic details of fluid flow and heat transfer in the con-

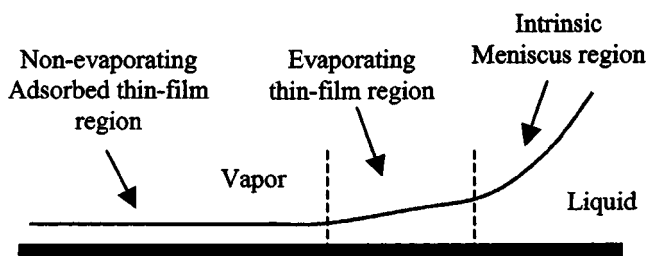


**Fig. 2 Details of an evaporating meniscus region**

tact line region of an evaporating curved liquid film in 1996. In their experiment, the evaporating film thickness profiles were measured optically using null ellipsometry and image analyzing interferometry. The pressure field was obtained from the thickness profiles using the augmented Young-Laplace equation. Using the liquid pressure field, the evaporative mass flux profile was obtained from a Kelvin-Clapeyron model for the local vapor pressure. An evaporating meniscus was formed in the circular experimental cell with octane as the working fluid.

## Objectives of the Present Work

The objectives of the present work are as follows:

1. Develop an apparatus to investigate stationary and moving liquid-vapor interface formed by a meniscus on a heated surface
2. Study the interface characteristics such as the advancing and receding contact angles through high speed photographs
3. Obtain quantitative information on the size and shape of the meniscus as a function of meniscus velocity and heater surface temperature
4. Obtain quantitative information on the heat transfer rates from the heated surface to the meniscus base as a function of water flow rate, meniscus velocity, and heater surface temperature

## Theoretical Analysis

The heat transfer in the meniscus region is modeled as consisting of three main features:

1. Transient heat conduction between the heater surface and the water
2. Evaporation of water along the receding liquid-vapor interface
3. Recirculation and mixing of the unevaporated water behind the advancing liquid-vapor interface with the incoming water

The recirculated and fresh incoming water streams are mixed as they flow behind the advancing liquid-vapor interface. The temperature of this mixed stream depends on the recirculation rate and the temperature of the incoming water.

Figure 3 identifies different flow regions considered in the present model. The inlet stream is identified as stream A, the mixed stream is identified as stream B, while stream C represents the water flowing over the heater surface encountering transient heat conduction, stream D is the fluid flow behind the receding interface, and stream E represents the evaporating water. Since the meniscus is stable, the inlet and the evaporating streams (A and E) are equal.

The transient heat transfer between the heater surface and water is dictated by the relative thermal diffusivities of water and the heated copper block. The instantaneous temperature of the interface of two semi-infinite mediums is given by Schneider [26] in the following:

$$T_{ins,s-w} = \frac{(k\rho c_p)_S^{1/2} T_{S,i} + (k\rho c_p)_W^{1/2} T_{W,i}}{(k\rho c_p)_S^{1/2} + (k\rho c_p)_W^{1/2}} \quad (1)$$

For an initial surface temperature of copper block of 108°C, and a water temperature of 100°C, using Eq. (1) we obtain  $T_{ins,s-w} = 107.65^\circ\text{C}$ . Because of the large thermal diffusivity of copper, the surface temperature is found to be close to the initial temperature of the copper block. Therefore, the interface temperature to be the same as the initial temperature of the copper block, and the transient heat transfer is modeled as the semi-infinite medium in water coming in contact with a constant temperature of the heater surface.

A detailed numerical study of a two-dimensional moving and evaporating meniscus was conducted by Mukherjee and Kandlikar

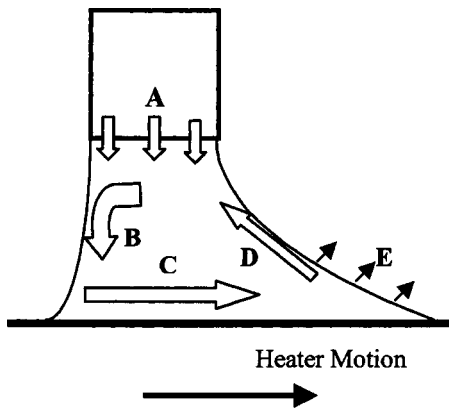


Fig. 3 Identifying various streams in a meniscus moving over a moving heater surface: (a) fresh water inlet, (b) recirculating mixed stream, (c) water stream in transient heat conduction with the heater surface, (d) water stream flowing behind the receding interface, and (e) evaporating vapor stream

[27]. The complete Navier-Stokes equations along with continuity and energy equations were solved. Circulation of liquid was observed inside the meniscus. Figure 4 shows the numerical results for recirculation of liquid inside the meniscus. The circulation pattern is seen to be similar to that shown in Fig. 3. The numerical results also showed that the heat transfer rate near the advancing liquid front was the highest due to transient conduction between the heater and the recirculated liquid. In the present work, heat transfer rates are experimentally measured over the entire meniscus region.

### Experimental Setup and Experimental Procedure

Figure 5 shows a schematic of the experimental setup with the water delivery system and the rotating heated copper block. The fluid delivery system is designed to deliver degassed and deionized water to the dispensing nozzle using gravitational head. The fluid delivery system includes a degassed water pouch, a flow meter with attached regulator valve, and a dispensing nozzle.

Figure 6 shows the schematic of the stationary test section used in the present study. A copper block with a 10 mm dia cylindrical extension is used as the heated surface. It is heated with the cartridge heater as shown. The top surface of the copper block is

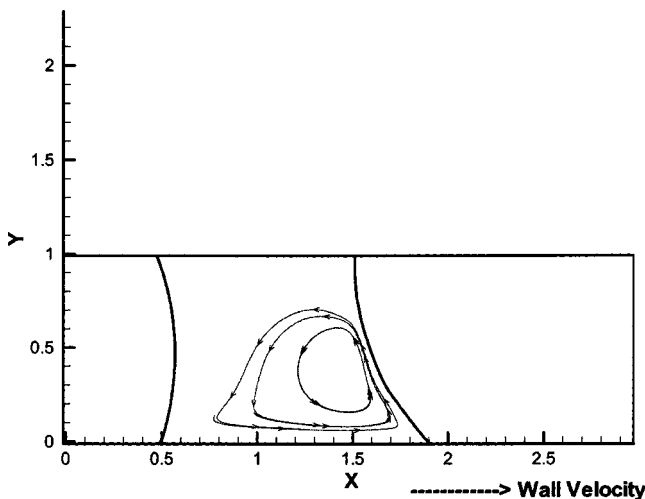


Fig. 4 Liquid circulation inside a moving and evaporating meniscus[27]

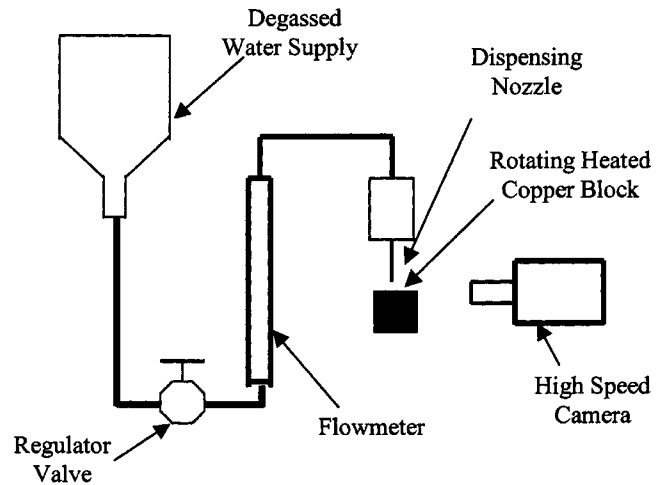


Fig. 5 Experimental setup

polished with 1  $\mu\text{m}$  slurry in the final stage of polishing. The polished surface prevents any boiling inside the meniscus by removing large-sized nucleation cavities. This allows a superheat of around 8–10°C without nucleation occurring inside the meniscus, thus providing a stable evaporating meniscus.

Figure 7 shows the schematic of a rotating test section. A copper block 37 mm in diameter and 63 mm long is placed on an insulating and support disk with four screw attachments to minimize the conduction losses. The top surface of the copper block is also polished with the 1  $\mu\text{m}$  slurry in the final stage of polishing. The assembly is then mounted on the shaft of an electric motor whose rotational speed can be closely controlled by supplying voltage from a digitally regulated power source. The test section is heated to the desired temperature by adjusting the temperature of an electric blower that blows hot air over the cylindrical surface of the copper block. The airflow is shielded from the heater surface as shown. A simple thermocouple probe is used to measure the temperature by stopping the rotation and inserting the probe in a hole made in the copper block. Because of the large mass of the copper block, the temperature does not change during the measurement. The copper surface is made level and true to the rotational axis so that the distance between the needle and the heater surface does not change as the motor turns the heater assembly. The needle is positioned at a certain radial distance from the center of rotation. This provides the necessary relative velocity as the

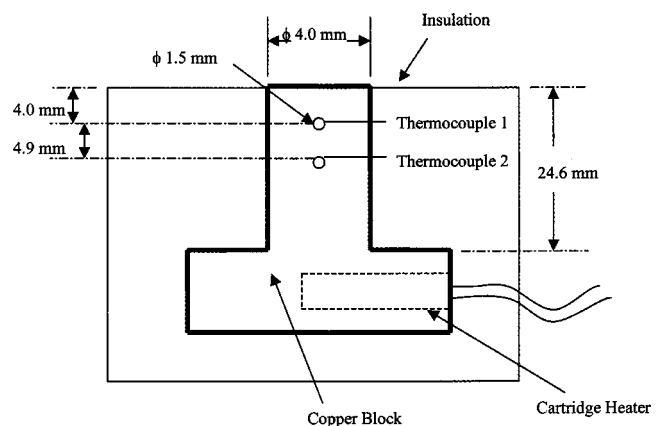


Fig. 6 Stationary test section schematic

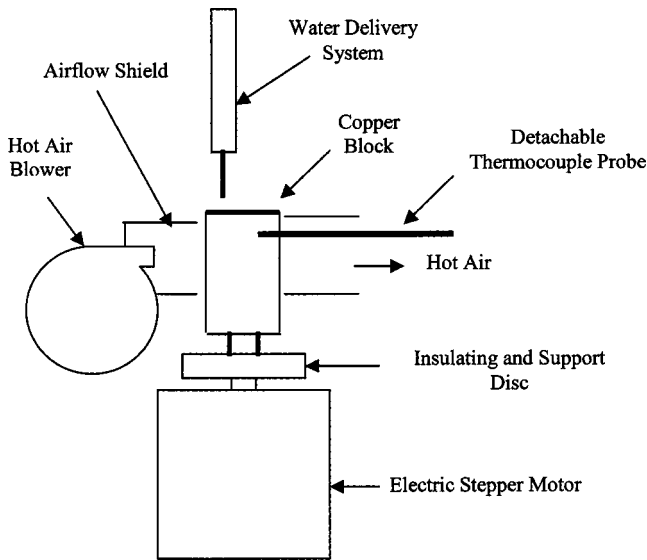


Fig. 7 Rotating test section schematic

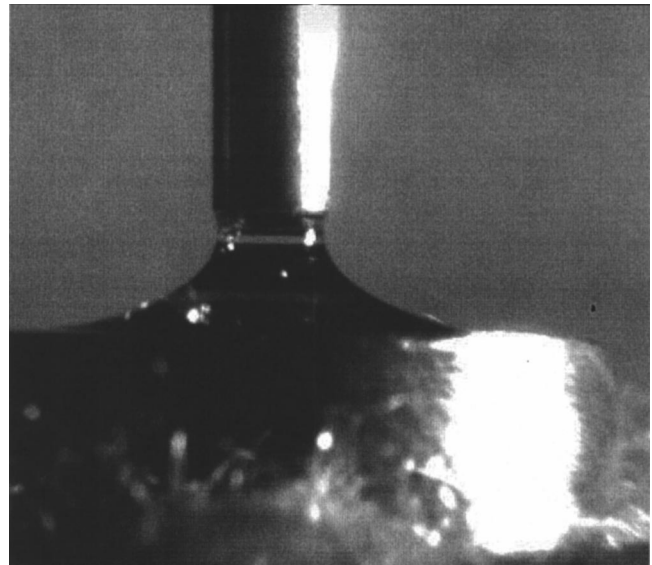


Fig. 8 Stationary meniscus at 108°C

heater surface turns. By adjusting the voltage to the electric motor, the rotational speed of the heated copper block can be closely controlled.

The images of the meniscus are obtained using a microscopic lens attached to two high-speed cameras that are both capable of recording frame rates of up to 8000 fps. The cameras are mounted on tripods and are located at an angle of 90 deg apart from each other. Using two cameras, we can obtain the width and length of the meniscus. Under stable operating conditions, all water supplied through the needle is evaporated; this provides accurate information regarding the heat transfer rate from the evaporating meniscus under various operating conditions.

### Experimental Uncertainties

The velocity of the rotating surface, the heater surface temperature, and the flow rate of water are three major parameters in this study. The flow rate of water is measured using a precision flow meter that is calibrated by actual measurement of flow using a chemical weighing scale over a 5 min period. The accuracy of

flow measurement is within  $\pm 2\%$ . The temperature measurement is accurate to within  $\pm 0.1^\circ\text{C}$ . The rotational speed is measured by calibrating the speed versus supply voltage. This is done in the vision software using the time steps with an indicator located on the rotating copper block. The error in measuring the distance of meniscus from the center of rotation is estimated to be 0.5 mm. The overall error in velocity measurement is estimated to be  $\pm 3\%$ .

The accuracy of combined advancing contact line angle and receding contact angle measurement is within  $\pm 1$  deg. The error in measuring the area of meniscus that is in contact with the heated surface is estimated to be  $\pm 8\%$ . The error in measuring the heat flux is estimated to be  $\pm 11\%$ .

### Results

The advancing and receding contact angles and heat transfer results for stationary and moving menisci are presented in this section. For the stationary meniscus, the contact angles are repre-

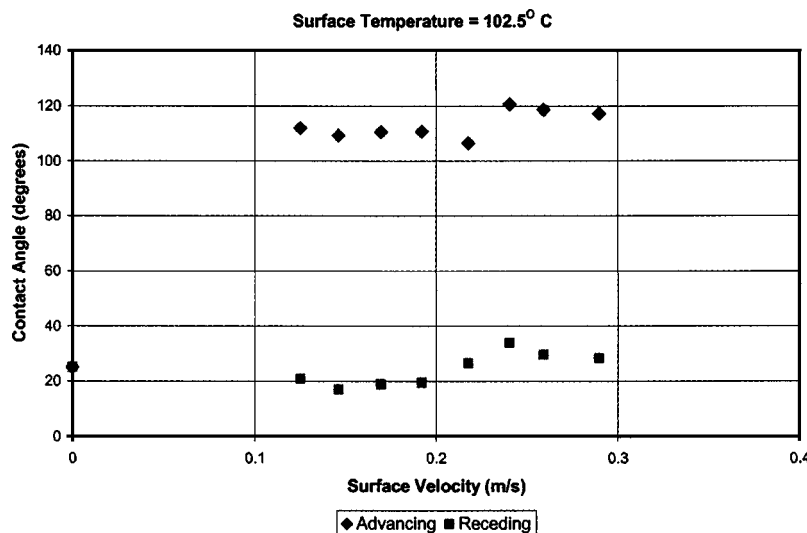


Fig. 9 Plot of receding and advancing contact angles versus surface velocity at 0.016 mL/min and surface temperature of 102.5°C

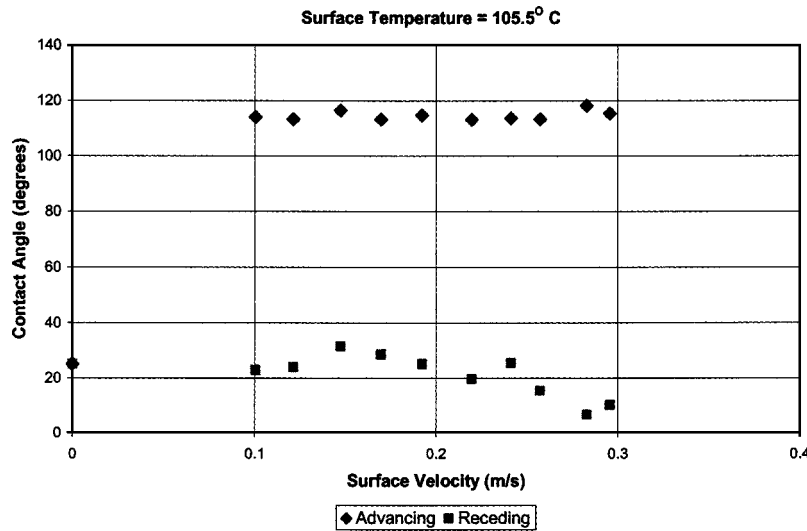


Fig. 10 Plot of receding and advancing contact angles versus surface velocity at 0.016 mL/min and surface temperature of 105.5°C

representative of the equilibrium contact angle. These are expected to fall between the advancing and the receding contact angle values. Figure 8 shows a typical stationary meniscus at 8°C superheat.

In the case of the rotating heater, the moving meniscus presents dynamic advancing and dynamic receding contact angles. These are measured from the images obtained with the high-speed camera. These images are transported into PRO-Engineering software program and then the respective angles are measured.

Figures 9–11 show the plots of the advancing and receding contact angles as a function of the relative surface velocity. The water mass flow rate is at a constant value of 0.016 mL/min. The surface temperatures are 102.5°C, 105.5°C, and 108°C, respectively. The zero velocity point corresponds to the stationary meniscus. For the stationary meniscus, the contact angle is found to be almost independent of the wall superheat.

In Fig. 9 as the surface velocity increases, the advancing and receding contact angles are found to be almost constant. In Fig. 10 as the surface velocity increases, the receding contact angle remains almost constant in the beginning but then decreases for higher velocities. In Fig. 11, as the relative surface velocity in-

creases, a larger scatter is seen in the contact angles. The operation became unstable at this temperature, with occasional meniscus breakage. The large scatter in contact angles seen in Fig. 11 are caused by interface instabilities set in by the high evaporation rate at the higher surface temperature of 108°C.

The surface heat flux under the meniscus area is calculated from the known water flow rate and the inlet temperature. Heat transferred in this region goes into heating the water from the inlet temperature to the saturation temperature of 100°C, and then evaporating it into steam at atmospheric pressure.

Thus  $q''$  is given by

$$q'' = \frac{[\dot{m}h_{fg} + \dot{m}C_p(100^\circ\text{C} - T_{in})]}{A} \quad (2)$$

where  $A$  is the footprint area of the meniscus.

The inlet temperature of water  $T_{in}$  is 20°C. The area for stationary meniscus is  $\pi r^2$ , and for the moving meniscus, the base surface area is calculated from the measured length, width, and shape of the footprint of the meniscus base.

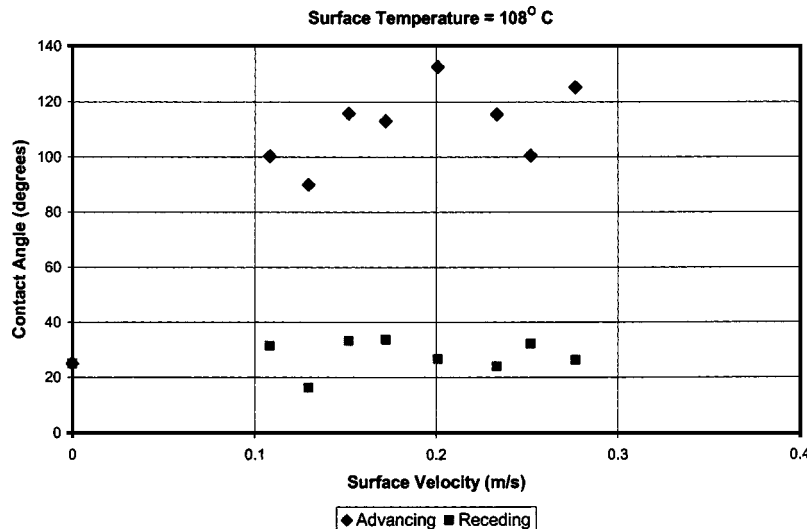


Fig. 11 Plot of receding and advancing contact angles versus surface velocity at 0.016 mL/min and surface temperature of 108°C

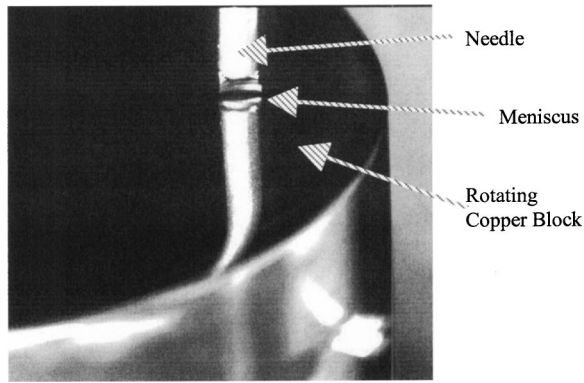


Fig. 12 Front view of moving meniscus

Figure 12 shows front view of the meniscus on the moving heated surface. The meniscus base width is measured at the contact line of the meniscus image and its reflection on the polished copper surface.

The length of the meniscus is obtained from Fig. 13, which shows the side view. The edge of the meniscus is found to be very clearly visible at both advancing and receding interfaces and no thin liquid films are observed. Presence of thin films in the contact

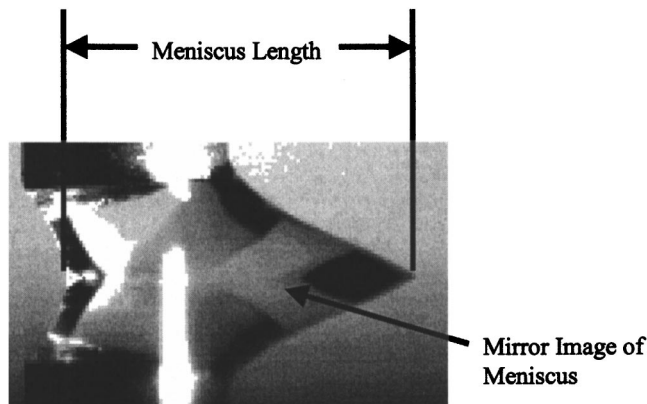


Fig. 13 Side view of moving meniscus

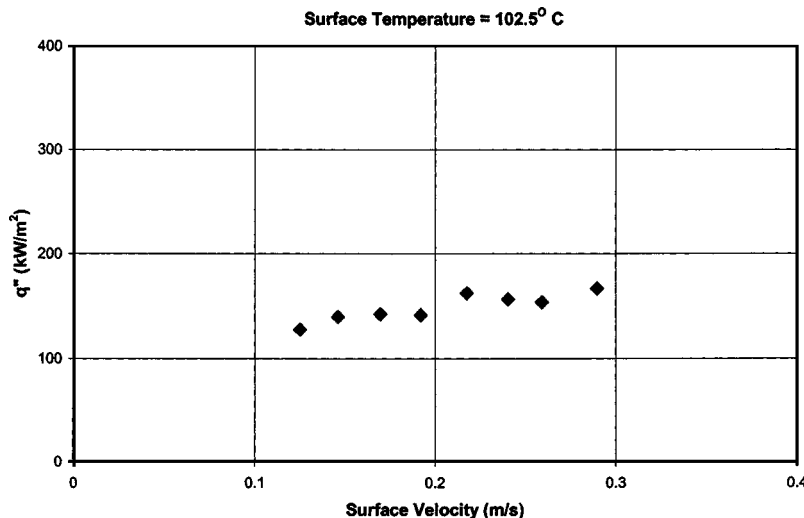


Fig. 14 Variation of heat flux with surface velocity at 0.016 mL/min for heater surface temperature of 102.5°C

regions is expected to show a change in reflected light from the copper surface. The top views of the receding interface shows a sharp and clear edge of the meniscus with no changes in reflectivity of light beyond it on the heater surface.

The meniscus base footprint is approximated as an ellipse with a major diameter given by its length and a minor diameter given by the width. The meniscus base area is thus calculated by measuring the length and width of the meniscus.

The heat transfer results are presented in terms of the measured heat flux as a function of surface velocity. Figures 14 and 15 show this variation for two different heater surface temperatures. It can be seen that there is a systematic dependence of heat flux on the surface velocity and surface temperature. At lower velocities, the heat flux is relatively insensitive to velocity. However, as the surface velocity increases the heat flux increases almost linearly as the transient conduction process becomes more efficient. Also, we note that the amount of scatter in the data increases with an increase in wall superheat, which is believed to be due to interface instability.

As seen in Figs. 16 and 17, the meniscus length decreases when the relative surface velocity increases because of increased transient conduction from the wall and subsequently higher evaporation rates.

Figure 18 shows the images of menisci for a constant surface temperature of 105.5°C and at a constant water mass flow rate of 0.016 mL/min with varying surface velocities. Note that the thin film region can be seen at the pointy edge in Figs. 18(a) and 18(b). This thin film region disappears from Fig. 18(c) to 18(e). The present visualization scheme allows for a detection of meniscus thickness of 1–2  $\mu\text{m}$ .

#### Comparison with Bubble Dynamics in Pool Boiling

In our experiments, for the relative surface velocity of 0.1 m/s and with 8°C excess temperature, the experimentally obtained heat flux value is about 150 kW/m<sup>2</sup>. The heat flux values taken from the boiling curve (e.g., Incropera [28]) for 110°C is 100 kW/m<sup>2</sup>. Thus, the advancing and receding motion of the meniscus provides heat transfer rates that are higher than the nucleate boiling values.

In the present experimental setup, the advancing and receding interfaces are exposed to air. Although the high evaporation rate at the receding interface is not expected to be affected by this, the presence of air is expected to increase the evaporation rate from the advancing interface due to the low partial pressure of water vapor in the air. A mass transfer analysis is performed to estimate

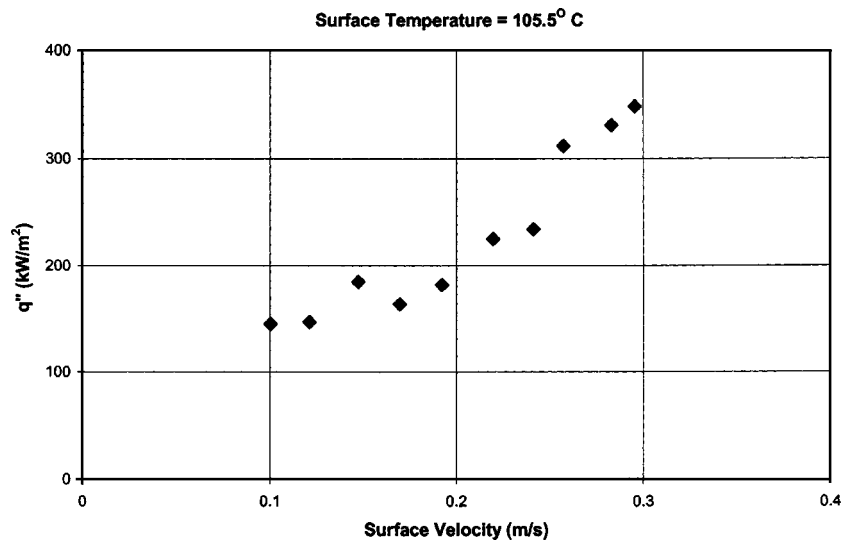


Fig. 15 Variation of heat flux with surface velocity at 0.016 mL/min for heater surface temperature of 105.5°C

this evaporative heat transfer rate from the advancing interface. The heat loss from the advancing interface to the air is estimated to be less than 10% of the total heat transfer rate under the present experimental conditions. In a pool boiling system, the heat transfer rate from the advancing interface will be lower as the interface is exposed to saturated steam and not the air. This could be one of the reasons why the experimental heat transfer rates obtained in the present work are higher than the pool boiling values. It is recommended that the surrounding air be replaced by a saturated vapor environment in future experiments to accurately simulate the pool boiling conditions.

Another reason for the discrepancy between the heat fluxes for meniscus and pool boiling system is that the present experimental system focuses only in the region bounded between the advancing and receding interfaces. In a boiling system, the actual liquid area contacting the heater surface would be quite different.

### Conclusions

An experimental investigation is conducted to study the characteristics of an evaporating meniscus on a smooth heated surface. The heat transfer characteristics are also investigated for both stationary and moving menisci. The study provides an important insight on the role of transient conduction around a nucleating bubble in pool boiling. The following conclusions are drawn from the present study.

1. For the stationary meniscus, the contact angle is almost independent of the wall superheat in the range of parameters investigated. It is seen to be almost constant at an angle of 26 deg for deionized water on polished copper surface.
2. In the case of a moving meniscus, as the surface velocity increases, the receding contact angle is found to vary whereas the

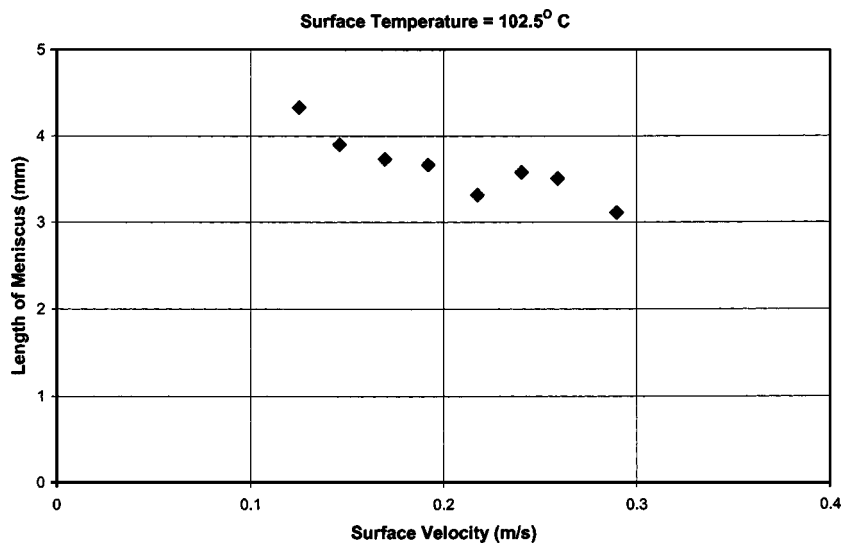


Fig. 16 Variation of meniscus length with surface velocity at 0.016 mL/min for heater surface temperature of 102.5°C

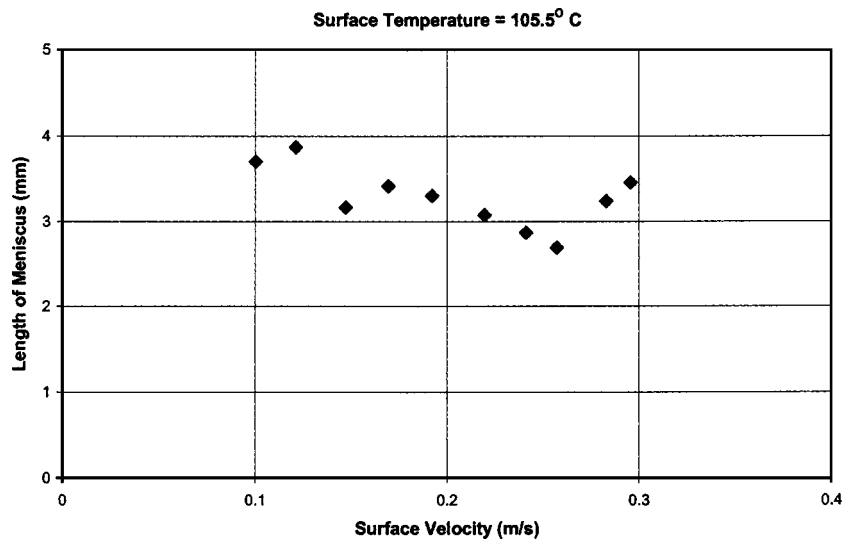


Fig. 17 Variation of meniscus length with surface velocity at 0.016 mL/min for heater surface temperature of 105.5°C

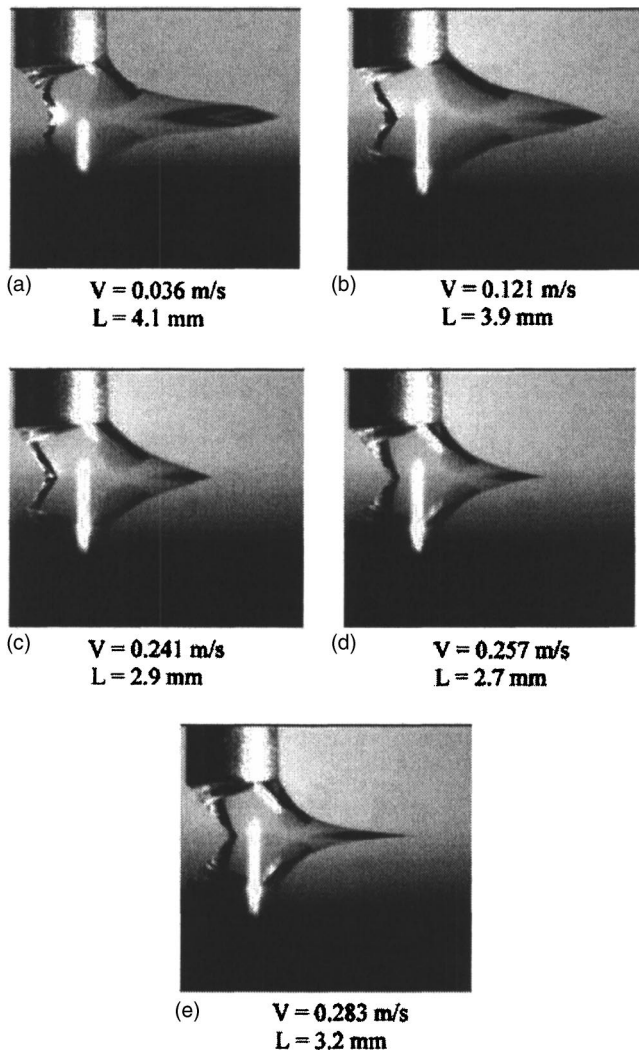


Fig. 18 Meniscus length  $L$  for different surface velocities at 0.016 mL/min at heater surface temperature of 105.5°C

advancing contact angle is found to remain almost constant. However, at high wall superheat of 108°C the meniscus became unstable and considerable scatter was observed in the contact angle measurements.

3. The heat flux at the meniscus footprint increases with the relative velocity.

4. The advancing and receding motion of the meniscus provides heat transfer rates that are higher than the average values during nucleate boiling.

#### Acknowledgment

All of the work was conducted in the Thermal Analysis Laboratory at RIT. The support provided by Rochester Institute of Technology is gratefully acknowledged.

#### Nomenclature

$A$  = area,  $\text{m}^2$   
 $c_p$  = specific heat of water at constant pressure,  $\text{J/kg}\cdot^\circ\text{C}$   
 $h_{fg}$  = latent heat of vaporization,  $\text{J/kg}$   
 $k$  = thermal conductivity,  $\text{W/m}\cdot^\circ\text{C}$   
 $L$  = distance between the advancing and receding fronts along the heater surface,  $\text{m}$   
 $\dot{m}$  = mass flow rate,  $\text{kg/s}$   
 $q''$  = heat flux,  $\text{W/m}^2$   
 $r$  = radius of stationary meniscus base  
 $T_{in}$  = water supply temperature,  $^\circ\text{C}$   
 $T_{w,i}$  = initial water temperature at the inlet to the transient conduction region,  $^\circ\text{C}$   
 $T_{s,i}$  = initial heater surface temperature at for the transient conduction, same as the heater block temperature,  $^\circ\text{C}$   
 $T_{ins,s-w}$  = instantaneous temperature of the interface of two semi-infinite medium,  $^\circ\text{C}$

#### Subscripts

$i$  = initial  
 $ins$  = instantaneous  
 $s$  = solid  
 $w$  = water

#### Greek Letters

$\alpha$  = thermal diffusivity,  $\text{m}^2/\text{s}$   
 $\rho$  = density,  $\text{kg/m}^3$

## References

- [1] Wayner, Jr., P. C., 1978, "The Effect of Thin Film Heat Transfer on Meniscus Profile and Capillary Pressure," *AIAA J.*, **17**(7), pp. 772–776.
- [2] Holm, F. W., and Golpen, S. P., 1979, "Heat Transfer in the Meniscus Thin Film Transition Region," *ASME J. Heat Transfer*, **101**, pp. 543–547.
- [3] Swanson, L. W., and Herdt, G. C., 1992, "Model of the Evaporating Meniscus in a Capillary Tube," *ASME J. Heat Transfer*, **114**(2), pp. 434–441.
- [4] Hallinan, K. P., Chebaro, H. C., Kim, S. J., and Chang, W. S., 1994, "Evaporation from an Extended Meniscus for Non-isothermal Interfacial Conditions," *J. Thermophys. Heat Transfer*, **8**(4), pp. 709–716.
- [5] Khurstalev, D., and Faghri, A., 1996, "Fluid Flow Effects in Evaporation From Liquid Vapor Meniscus," *ASME J. Heat Transfer*, **118**(3), pp. 725–731.
- [6] Kim, I. Y., and Wayner, Jr., P. C., 1996, "Shape of an Evaporating Completely Wetting Extended Meniscus," *J. Thermophys. Heat Transfer*, **10**(2), pp. 320–326.
- [7] DasGupta, S., Schonberg, J. A., and Wayner, P. C., 1993, "Investigation of an Evaporating Extended Meniscus Based on the Augmented Young-Laplace Equation," *ASME J. Heat Transfer*, **115**, pp. 201–208.
- [8] Derjaguin, B. V., 1940, "A Theory of Capillary Condensation in the Pores of Sorbents and Other Capillary Phenomena Taking Into Account the Disjoining Action of Polymolecular Liquid Films," *Acta Physicochim. URSS*, **12**(1), pp. 181–200.
- [9] Derjaguin, B. V., Nerpin, S. V., and Churaev, N. V., 1965, "Effect of Film Transfer Upon Evaporating Liquids From Capillaries," *RILEM Bull.*, **29**(1), pp. 93–98.
- [10] Lay, J. H., and Dhir, V. K., 1995, "Shape of a Vapor Stem During Nucleate Boiling of Saturated Liquids," *ASME J. Heat Transfer*, **117**, pp. 394–401.
- [11] Nikolayev, V. S., and Beysens, D. A., 1999, "Boiling Crisis and Non-equilibrium Drying Transitions," *Europhys. Lett.*, **47**(3), pp. 345–351.
- [12] Pierret, R. F., 1996, *Semiconductor Device Fundamentals, Solutions Manual*, Addison-Wesley, Reading, MA, pp. 6.12
- [13] Potash, Jr., M., and Wayner, Jr., P. C., 1972, "Evaporation From a Two-Dimensional Extended Meniscus," *Int. J. Heat Mass Transfer*, **15**, pp. 1851–1863.
- [14] Schonberg, J. A., 1995, "An Augmented Young-Laplace Model of an Evaporating Meniscus in a Microchannel With High Heat Flux," *Experimental Thermal and Fluid Science 1995*, Elsevier Science, New York, pp. 163–170.
- [15] Sefiane, K., Benielli, D., and Steinchen, A., 1998, "A New Mechanism for Pool Boiling Crisis, Recoil Instability, and Contact Angle Influence," *Colloids Surf.*, **A**, **142**, pp. 361–373.
- [16] Shoji, M., Mori, Y. H., and Maruyama, S., 1999, Representation of Solid-Liquid-Vapor Phase Interactions, *Handbook of Phase Change-Boiling and Condensation*, S. G. Kandlikar, M. Shoji, and V. K. Dhir, eds. Taylor and Francis, Philadelphia, Chap. 6, Sec. 2.2.6.
- [17] Son, G., Dhir, V. K., and Ramanajapu, N., 1999, "Dynamics and Heat Transfer Associated With a Single Bubble During Nucleate Boiling on a Horizontal Surface," *ASME J. Heat Transfer*, **121**, pp. 623–631.
- [18] Sujjanani, M., Wayner, Jr., P. C., 1992, "Transport Processes And Interfacial Phenomena in an Evaporating Meniscus," *Chem. Eng. Commun.*, **118**, pp. 89.
- [19] Wayner, Jr., P. C., 1991, "The Effect of Interfacial Mass Transport in Thin Liquid Films," *Colloids Surf.*, **52**, pp. 71–84.
- [20] Wayner, P. C., Jr., 1992, "Evaporation and Stress in the Contact Line Region," *Proc. Conference on Pool and External Flow Boiling*, Santa Barbara, V. K. Dhir, and A. E. Bergles, eds., Engineering Foundation, New York, pp. 251–256.
- [21] Wayner, Jr., P. C., 1994, "Thermal and Mechanical Effects in the Spreading of a Liquid Film Due to a Change in the Apparent Finite Contact Angle," *ASME J. Heat Transfer*, **116**, pp. 938–945.
- [22] Wayner, P. C., Jr., DasGupta, S., and Schonberg, J. F., 1991, "Effect of Interfacial Forces on Evaporating Heat Transfer in a Meniscus," Technical Report WL-TR-91, Wright-Patterson AFB, Ohio.
- [23] Wayner, Jr., P. C., Kao, Y. K., and Lacroix, L. V., 1976, "The Interline Heat Transfer Coefficient of an Evaporating Wetting Film," *Int. J. Heat Mass Transfer*, **19**(2), pp. 487–492.
- [24] Kandlikar, S. G., and Kuan, W. K., 2003, "Circular Evaporating Meniscus: A New Way to Study Heat Transfer Mechanism During Nucleate Boiling," 5th International Conference on Boiling Heat Transfer 2003, Jamaica, May 4–8.
- [25] Kandlikar, S. G., and Kuan, W. K., 2003, "Heat Transfer From a Moving and Evaporating Meniscus on a Heated Surface," ASME Summer Heat Transfer Conference 2003, Las Vegas, July 20–23.
- [26] Schneider, P. J., 1955, *Conduction Heat Transfer*, Addison-Wesley, Reading, MA.
- [27] Mukherjee, A., and Kandlikar, S. G., 2004, "Numerical Study of an Evaporating Meniscus on a Moving Heated Surface," ASME Summer Heat Transfer Conference 2004, Charlotte NC, July 11–15, HT-FED2004-56678.
- [28] Incropera, F. P., and DeWitt, D. P., 2002, *Pool Boiling, Fundamentals of Heat and Mass Transfer*, John Wiley and Sons, Inc., New York, Chap. 10, Sec. 10.3.2.